

# Enhanced diffusion of a tracer particle in a lattice model of a crowded active system

Leila Abbaspour<sup>1,\*</sup> and Stefan Klumpp<sup>1,†</sup>

<sup>1</sup>*Institute for the Dynamics of Complex Systems, Georg August University of Göttingen,  
Friedrich-Hund-Platz 1, 37077 Göttingen, Germany.*

(Dated: June 18, 2020)

Living systems at the sub-cellular, cellular, and multi-cellular level are often crowded systems that contain active particles. The active motion of these particles can also propel passive particles, which typically results in enhanced effective diffusion of the passive particles. Here we study the diffusion of a passive tracer particle in such a dense system of active crowders using a minimal lattice model incorporating particles pushing each other. We show that the model exhibits several regimes of motility and quantify the enhanced diffusion as a function of density and activity of the active crowders. Moreover, we demonstrate an interplay of tracer diffusion and clustering of active particles, which suppresses the enhanced diffusion. Simulations of mixtures of passive and active crowders show that a rather small fraction of active particles is sufficient for the observation of enhanced diffusion.

## I. INTRODUCTION

The behavior of individual particles within a crowded environment is influenced by the complex collective behavior of the surrounding particles [1–4]. Indeed, many biological systems are densely packed. Molecular systems in the cytoplasm of cells [1, 5], colonies of bacteria [6], bio-films [7], and tissues [8] are a few examples. Often, the crowded environment contains active particles that are driven out of equilibrium due to the local injection and dissipation of energy. On the molecular scale these active particles may be molecular motors pulling cargoes through cytoplasm and 'stirring it' [9–11] or enzymes exhibiting enhanced diffusion [12, 13], on the cellular scale, these could be self-propelled cells swimming in a suspension or moving through a tissue or a colony of cells [14, 15]. This means that detailed balance is not fulfilled in these systems, so they cannot be described by equilibrium statistical mechanics.

The observation of individual 'probe' or 'tracer' particles within such a system provides a method to quantify crowding effects as well as to probe for the degree of crowding if this is difficult to determine directly. Such probes include the diffusion of the tracer particle [16, 17] as well as specific chemical reactions or conformational changes such as the compaction of a polymer chain as measured by FRET-probes at the two ends of the polymer [18, 19].

Diffusion of molecules and particles in complex environments has been studied on a range of length scales and the complex environment can give rise to dynamic phenomena such as anomalous diffusion [20, 21]. Specifically, diffusion of a passive tracer particle in an active system has been studied in various experimental and theoretical model systems. Notably, Wu and Libchaber [22] studied the trajectories of polystyrene beads in a suspension of swimming bacteria and observed enhanced diffusion of the beads.

Such enhanced diffusion has been studied extensively, both theoretically [23–30] and experimentally [25, 31–37]. Extensions of the simplest system include 3 dimensional systems [36], the presence of obstacles [34] and confinement, and effective interaction between passive particles [38].

Interactions between particles in suspension can be complex and generally involve hydrodynamic interactions in addition to simple excluded volume and particle-particle collisions. Therefore, simplified minimal models systems can help to advance our understanding of the role of active processes. Both continuum models [39] and lattice models [40, 41] have been used for that purpose. Enhanced diffusion of a tracer in a crowded active system has been observed in models with and without hydrodynamic interactions [25, 42]. Following this approach, we study a minimal lattice model incorporating particle-particle collisions as well as different diffusion coefficients of different particle types to investigate the effect of activity and density of crowders on tracer diffusion. We quantify the enhanced diffusion as a function of these parameters and relate the observed tracer diffusion to clustering of active particles. Finally, we generalize our analysis to the case of a binary mixture of active and passive particles. Our results indicate how the interplay between activity and density of crowders can lead to significant enhancement of the diffusion of a tracer, but also limits that enhancement through clustering of the active particles.

---

\* [Leila.abbaspour@theorie.physik.uni-goettingen.de](mailto:Leila.abbaspour@theorie.physik.uni-goettingen.de)

† [Stefan.klumpp@phys.uni-goettingen.de](mailto:Stefan.klumpp@phys.uni-goettingen.de)

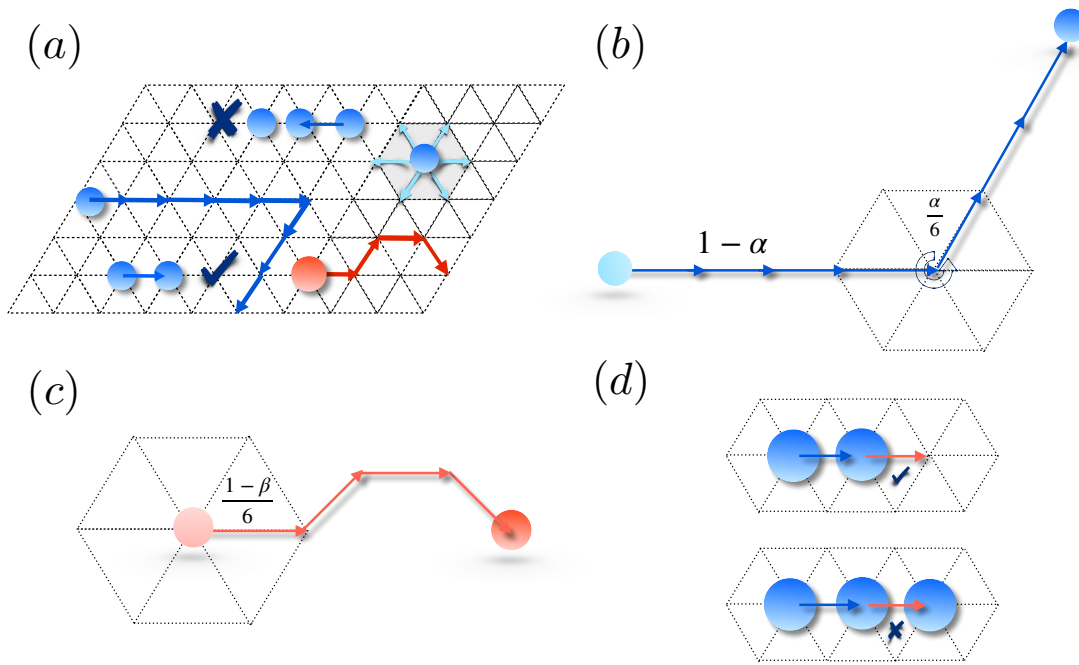


FIG. 1. Lattice model of a dense system of active particles (blue) containing a passive tracer particle (red). a) Overview of the model on a hexagonal lattice. b) Active particles perform run and tumble motion and move persistently in the same direction with probability  $1 - \alpha$  and randomize that direction (tumble) with probability  $\alpha$  (i.e.,  $\alpha/6$  for each direction). c) The passive tracer particle (red) performs a simple random walk, its diffusion coefficient is modulated by the parameter  $\beta$ . d) Collision rules among particles.

## II. MODEL

We consider a hexagonal lattice (see Fig. 1(a)) in two dimensions, consisting of  $M = 256 \times 256$  sites, with periodic boundary conditions. There are in total  $N$  particles on the lattice, of which  $N_a = \chi_A N$  are active and can self-propel following a simplified run and tumble motion, and the rest are passive and exhibit diffusive behaviour. We define  $\rho$  as the number density of the system, which is defined as the total number of particles divided by the number of lattice sites.

For updating the position of all particles at each time step,  $N$  random actions take place in the system. A particle may be picked more than once in one single time step, giving rise to fluctuation of its speed. On average, however, all particles are picked equally often.

The active particles have run-and-tumble dynamics, where they move persistently in one direction (initially chosen at random), and then reorient with a tumbling probability  $\alpha$ , resulting in long directed runs with abrupt turns. At each time step, the active particle moves in the same direction as in its last step with probability  $1 - \alpha$ , and tumbles to choose a new direction with probability  $\alpha/6$ . For instance, for  $\alpha = 0.001$ , the active particle takes, on average, 1000 persistent steps in the same direction, and then tumbles and chooses one out of the six possible directions with equal probability (see Fig. 1(b)). In the case of passive particles we set  $\alpha = 1$ : the particle reorients at each time step and therefore steps to each site with a probability of  $1/6$ . Since our aim is to study the effect of active particles on the overall motion of a passive particle, we put (at least) one passive ‘tracer’ in the system, which in general has a different Brownian diffusion coefficient set by a parameter  $\beta$ . The tracer steps to each neighbour site with probability  $(1 - \beta)/6$ , with  $0 \leq \beta \leq 1$  as shown in Fig. 1(c). When  $\beta = 0$  the tracer has the same dynamics as the passive crowd. As  $\beta$  increases, the tracer diffuses more slowly and in the limiting case of  $\beta = 1$ , it can only move by being pushed by its neighbors.

We now define collision rules among the particles. We use a modified exclusion rule, which in addition to ensuring that each site is occupied by at most one particle also allows for particles pushing each other. In each stepping attempt of a particle, we check whether the target site on the lattice is empty or occupied. If it is empty, then the particle is allowed to update its position, as described above. If the site is occupied, then there are two possibilities depending on the second neighbor site of the particle in the same direction. If the latter site is empty, the stepping particle pushes the particle in the target site to the second neighbor site and moves to the target site itself. Otherwise, the update

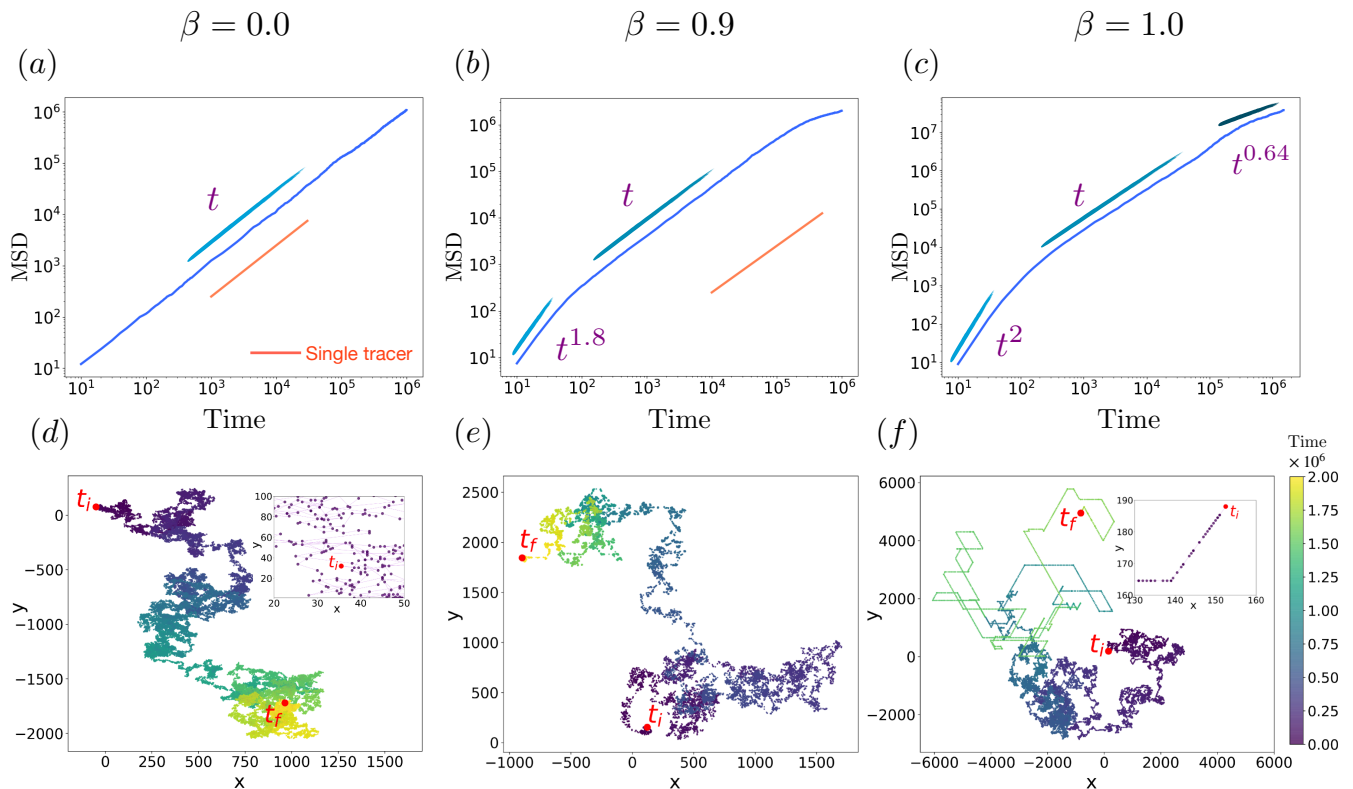


FIG. 2. Diffusion of tracer particles with different diffusion coefficients in a system of active crowders. (a-c) The mean square displacement shows diffusive motion for  $\beta = 0$  and anomalous diffusion for  $\beta = 0.9, 1$ . The red lines indicate the diffusive motion of the tracer in an otherwise empty lattice, in (c) the tracer would not move in that case. (d-f) show trajectories, the insets show the trajectories at the early stages. Each column corresponds to the value of  $\beta$  indicated above it. The other parameters are  $\rho = 0.025$ ,  $\alpha = 0.0001$ .

is rejected (see Fig. 1(d)). Note that there is no alignment interaction between particles in the pushing process. All simulations described in the following were run for  $10^6$  time steps with 1000 realizations of each condition.

### III. RESULTS

#### A. Tracer in a purely active system

##### 1. Mean square displacement

We first discuss the results for a passive tracer particle in the presence of only active crowders (i.e.,  $N_a = N$  or  $\chi_A \approx 1$ ). We considered densities in the range of  $0.01 \leq \rho \leq 0.4$  and the tumbling probability of active particles between  $0.0001 \leq \alpha < 1$ .

We begin our analysis by evaluating the mean square displacement (MSD) of the tracer particles. We note that for Brownian motion, the MSD is given by,  $\langle (\Delta r)^2 \rangle = 2dDt$ , where  $\Delta r$  is the displacement of a particle in a given time interval of  $t$ ,  $d$  is the spatial dimension (which is 2 in our case),  $D$  is the diffusion coefficient, and  $\langle \cdot \rangle$  denotes an ensemble average. So-called anomalous diffusion is characterised by an MSD  $\langle (\Delta r)^2 \rangle \sim t^\gamma$ , where  $\gamma \neq 1$  is a real positive number that classifies the different types of diffusion: sub-diffusion for  $0 < \gamma < 1$  and, super-diffusion for  $\gamma > 1$  (where  $\gamma = 2$  gives rise to ballistic motion).

In Figs. 2(a)-(f), we have plotted the MSD and corresponding trajectories as a function of time for the three cases of  $\beta = 0, 0.9$ , and 1. In all three cases, the density and the tumbling probability of crowders are the same:  $\rho = 0.025$  and  $\alpha = 0.0001$ . For a purely passive Brownian tracer with  $\beta = 0$  (Figs. 2(a) and (d)), the tracer shows normal

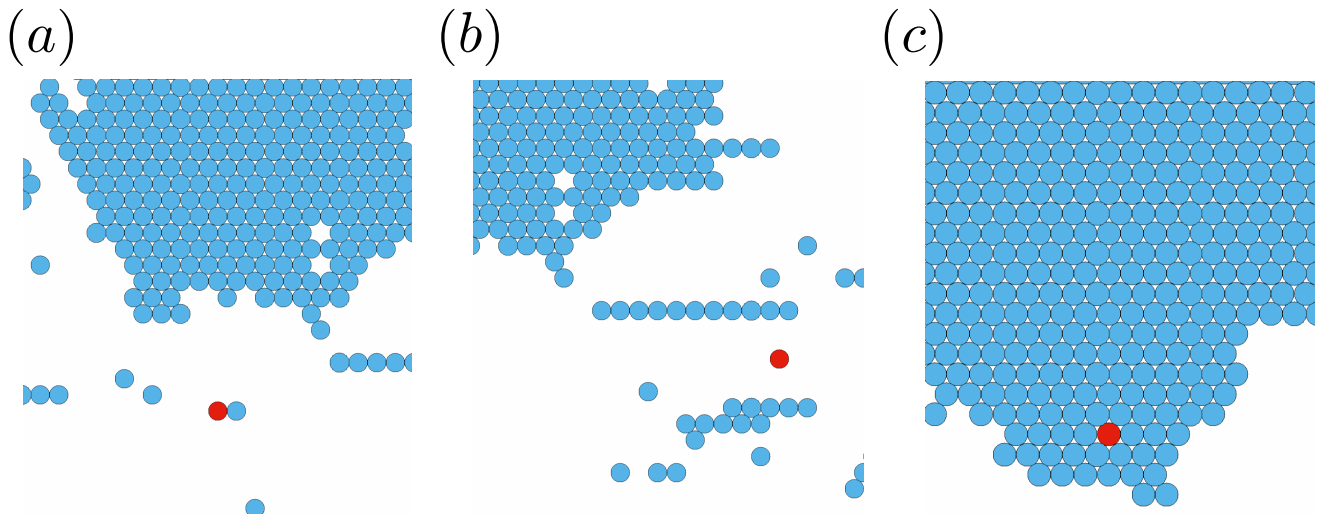


FIG. 3. Snapshots of the simulation for  $\rho = 0.1$  and  $\alpha = 0.0001$ : the active particles are shown in blue and the tracer particle in red. a) The tracer (red) is next to an active particle (blue), which pushes it. b) The tracer is trapped in empty space. c) The tracer is trapped by active particles.

diffusion, with an MSD that is linear in time throughout the simulation. The trajectory is erratic at both long and short time (Figs. 2(d) and its inset, respectively).

It is useful to compare the diffusion coefficient of the tracer in this system to that of a passive tracer in the absence of active crowders. For a single passive particle on an isotropic lattice, the diffusion coefficient is given by  $D_0 = (\kappa/2d)a^2\lambda$ , where  $a$  is the lattice constant,  $\kappa$  is the coordination number (the number of neighbour sites allowed for a jump), and  $\lambda$  is the stepping rate to the nearest neighbour site [43]. In our model  $a = 1$ ,  $\kappa = 6$ ,  $d = 2$ , and  $\lambda = \frac{1-\beta}{6}$ , leading to

$$D_0 = \frac{1-\beta}{4}. \quad (1)$$

Thus, for  $\beta = 0$  we find  $D_0 = 1/4$ , which as shown in Fig. 2(a) (red line) indicates that the diffusion coefficient of our tracer particle is enhanced due to presence of active crowders.

For  $\beta = 0.9$  and  $\beta = 1$ , by contrast, we can identify several diffusive regimes. A slow tracer with  $\beta = 0.9$  initially undergoes super-diffusion (Fig. 2(b)) as it remains in front of an active particle over an extended period of time (see Fig. 3(a)). The tracer inherits the direction of an individual active particle which drives it forward. This effect can also be seen in the inset of Fig. 2(e), in which this directed motion yields a straight line. The observed diffusion exponent  $\gamma$  at short time is found to be 1.8, which is close to the ballistic regime with  $\gamma = 2$ . After a longer time, diffusive motion is recovered, with erratic trajectories similar to those for  $\beta = 0$ .

Finally, Figs. 2(c) and (f) show the case where the passive tracer does not move by itself and only moves when pushed by an adjacent active particle. Initially, the tracer fully inherits the direction and the speed of the active particle that pushes it (Fig. 2(f) inset). Since there is only self-propulsion,  $\gamma$  is exactly 2. For an intermediate time, diffusive behaviour is recovered. Then after some time, the motion becomes remarkably less random, exhibiting long directed paths and pauses, as depicted in the trajectory in Fig. 2(f). Correspondingly, the exponent of the MSD is reduced to  $\gamma \sim 0.64$ , indicating a sub-diffusive behaviour. Inspection of snapshots of the lattice (Figs. 3(b) and (c)) show that during the pauses, the tracer is either trapped in an empty region of the lattice and thus cannot be moved, or in a cluster of active particles, within which it is also immobilized. This observation indicates that, in this case, the environment in which the tracer diffuses through changes from a homogeneous environment, to coexistence of a dilute phase and clusters of active particles. Cluster formation will be discussed in more detail below.

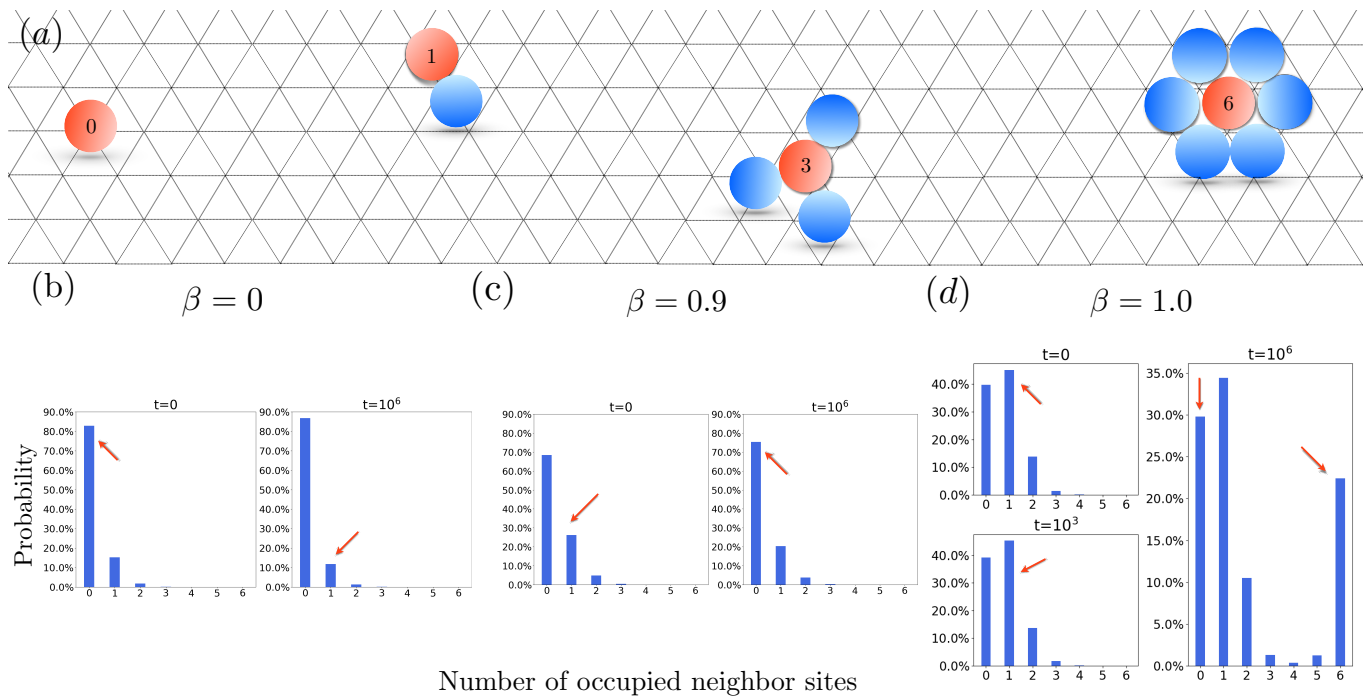


FIG. 4. Trapping analysis. a) The sketch shows the tracer (red) surrounded by different number of active particles (blue). (b), (c) and (d) show the probability that  $N_n$ , neighbor sites are occupied (for  $n = 0, \dots, 6$ ). The red arrows indicate the numbers of occupied neighbors most relevant for the different regimes in the MSD plots in Fig. 2.

## 2. Neighbour site occupation and trapping

To quantify the effect of trapping on the motion of a tracer, we define a trapping parameter  $N_n$ , which characterizes the occupation of the six nearest neighbour sites of the tracer (see Fig. 4 (a)). Thus,  $0 \leq N_n \leq 6$ , with  $N_n = 0$  indicating that the tracer has no neighbouring particle and  $N_n = 6$  is the fully trapped state. When  $N_n = 0$ , the tracer with  $\beta = 1$  is essentially trapped by the empty space and becomes immobile, while tracers with  $\beta = 0$  and  $\beta = 0.9$  diffuse on their own. In the fully occupied state ( $N_n = 6$ ), the tracer is immobile for all the cases.  $N_n = 1$  results in persistent directed motion of the tracer if the neighboring active particle moves to the site of the tracer and  $1 - \beta < 1 - \alpha$ , as the active particle then pushes the tracer for multiple steps.

For the two cases  $\beta = 0$  and  $\beta = 0.9$ , the histograms of  $N_n$  do not vary significantly over time, with the probability of having no neighbors being the largest (Figs. 4(b) and (c)). As expected, the probability of having a single neighbor ( $N_n = 1$ ) is higher for  $\beta = 0.9$  than  $\beta = 0$ , in agreement with the observed directed motion. For  $\beta = 1$ ,  $N_n = 1$  is the most probable configuration at all times. However, the histogram remarkably broadens over time and becomes bi-modal at long times, with  $N_n = 0$  and  $N_n = 6$  occurring (almost) equally frequently. This means that the three most likely configurations are those that lead to directed motion ( $N_n = 1$ ), trapping in empty space ( $N_n = 0$ ) or trapping in a cluster ( $N_n = 6$ ), which together explain the range of motion observed in Fig. 2(f).

## 3. Effective diffusion coefficient at large times

We have observed above that diffusion of the tracer is enhanced in the bath of active particles compared to the tracer on its own. To study this further, in Fig. 5, we plot the diffusion coefficient at large times as a function of density, focusing on the case  $\beta = 0.9$ . The simulation was performed for a system with  $\chi_A = 1$ , and different values of  $\alpha$ . Remarkably, the effective diffusion coefficient has a 50-fold increase when in the active bath, compared to the diffusion coefficient of an isolated tracer. Even at a low density ( $\rho \approx 0.01$ ) of active crowders, the diffusion coefficient of the tracer is substantially greater than in the absence of active crowders, implying a strong effect of being pushed by active particles.

Since the diffusion coefficient of a single passive tracer is a small constant in the absence of crowders and goes to zero in the presence of a high density of crowders, the relative diffusion coefficient is expected to be a non-monotonic

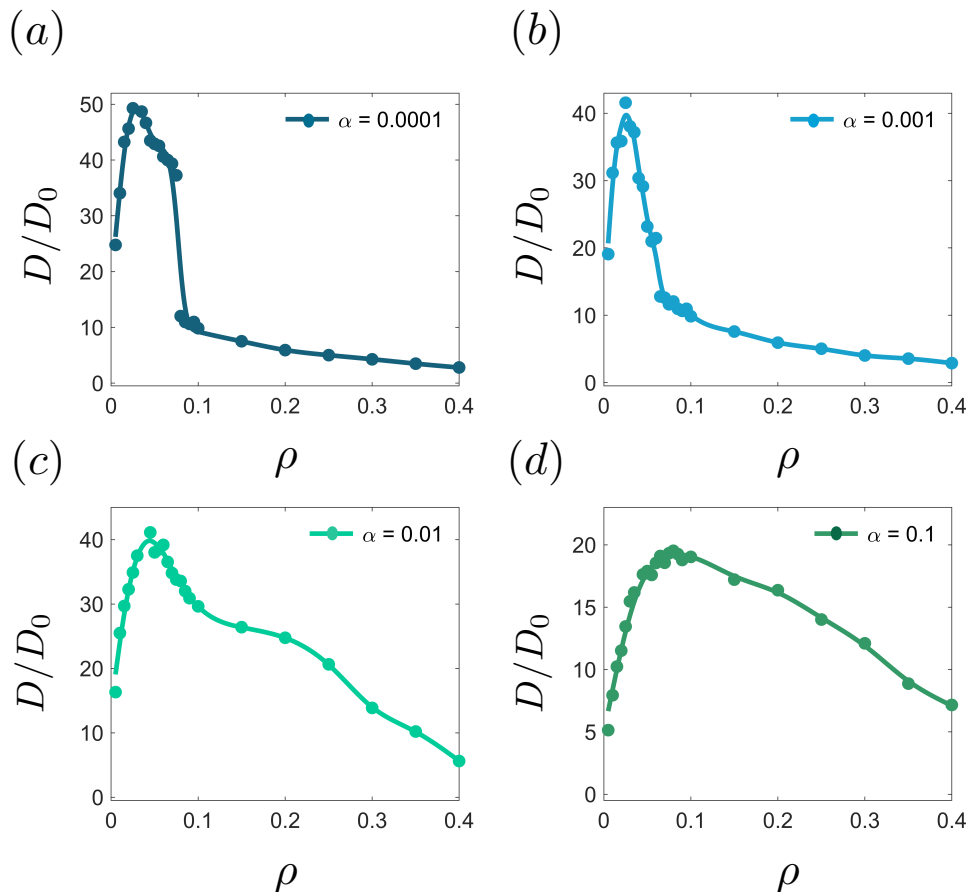


FIG. 5. The relative diffusion coefficient of a tracer with  $\beta = 0.9$ , normalized to the diffusion constant  $D_0$  of an isolated tracer.

function of the density. Furthermore, the form of this dependence should also vary with the tumbling probability. The plots in Fig. 5 show a clear density dependence of the diffusion coefficient. The diffusion coefficient is sharply enhanced when the density of active particles is increased from zero, then decreases after a pronounced peak. Clearly, the density of the system greatly affects the diffusion coefficient of the tracer. To further investigate this effect, we come back to the observation of cluster formation.

#### 4. Cluster formation

To analyze clustering, we define a cluster as a collection of at least six particles 'sticking together', i.e. being connected via mutual nearest neighbors. Particles without nearest neighbor or connected to fewer particles are considered as belonging to the gas phase. Clusters are identified with the data analysis framework Freud [44]. We measured the average cluster size,  $C_s$ , as the average number of particles in a cluster over 1000 different realizations of the simulation. Figs. 6(a) and (b) show the time evolution of  $C_s$  for different densities and for  $\alpha = 0.001$  and 0.0001, respectively. As can be seen in Figs. 6(a) and (b), cluster formation is accelerated by increasing the density of crowders.

In Fig. 6(c) and (d), we plotted the fraction of particles detected within clusters,  $\phi_c$ , as seen in the last snapshot of the simulation which provides an estimate of the fraction of particles assembled in the clusters.  $\phi_c$  can be described by  $(N_c \times C_s)/N$ , where  $N_c$  is the average number of clusters. As a function of the density,  $\phi_c$  shows a clear transition from a state in which a very small fraction of particles are in the clusters to a state where almost all particles are in clusters.

To relate clustering to the tracer diffusion discussed before, we indicate with the vertical dashed lines the density at which the tracer's diffusion coefficient for the given tumbling probability is maximal. These lines fall near the transition to global clustering, suggesting an intimate relation of the decline in diffusion to the onset of phase separation. When the active crowders start to form clusters, there is coexistence of a dilute gas phase and clusters of active particles and

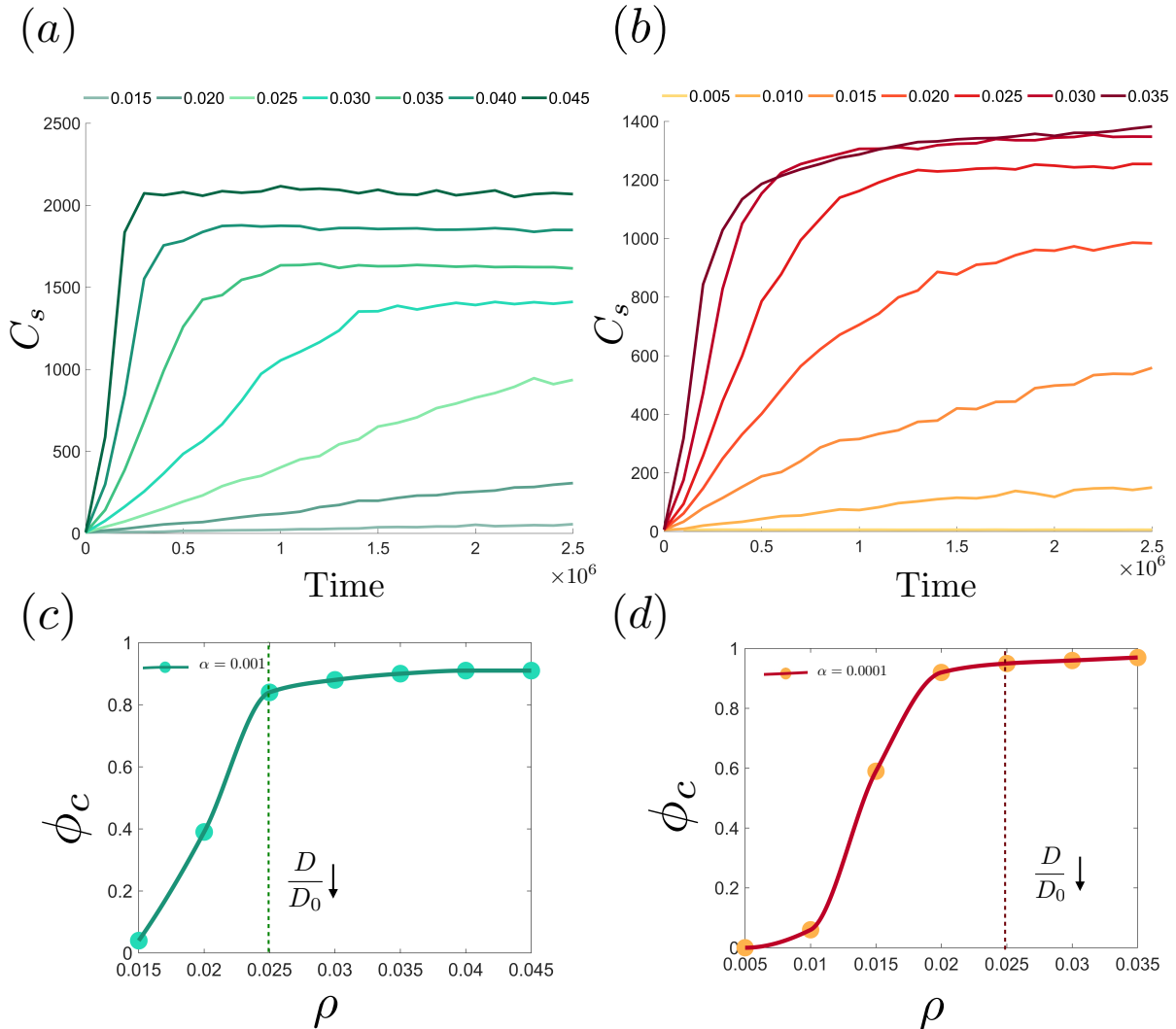


FIG. 6. Cluster analysis: a) and b) Average cluster size as a function of time (averaged over 1000 realizations) for different densities. c) and d) Fraction of particles assembled in clusters in the last snap shot of simulation for the same densities. The dashed lines mark the density in which the tracer exhibits the maximum diffusion coefficient. a,c)  $\alpha = 0.001$ , b,d)  $\alpha = 0.0001$ .

the probability of active crowdors being in the dilute phase decreases as long as the cluster size increases. Consequently, the diffusion coefficient of the tracer decreases as there are fewer and fewer active crowdors in the dilute phase to push the tracer and enhance its diffusion.

## B. Binary Mixture

Finally, we consider a binary mixture of active and passive crowdors, with  $\chi_A + \chi_P = 1$  where  $\chi_P$  is the fraction of passive particles. We tracked the effect of the three control parameters  $\chi_A$ ,  $\alpha$  and  $\rho$  on the diffusion coefficient of a tracer particle with  $\beta = 0.9$ . Adding passive particles into a purely active system changes not only the directionality imposed by collisions (due to pushing by the active particles), but also alters the global dynamics in a subtle way, specifically the dynamics of clustering. In the example shown in Fig. 7 with a fixed low density of crowdors, an increase of the fraction of active crowdors above 0.5 leads to a strong clustering signature both in the average cluster size  $C_s$  and in the fraction  $\phi_c$  of particles within clusters (inset). The cluster size  $C_s$  shows biphasic growth for large fractions of active crowdors with first rapid increase in the cluster size and then a much slower second phase, which appears to be more pronounced and slower for the largest active crowder fractions. Put differently, replacing some of the active crowdors with passive particles delays the phase separation (compare the cases  $\chi_A = 1$  and  $\chi_A = 0.75$

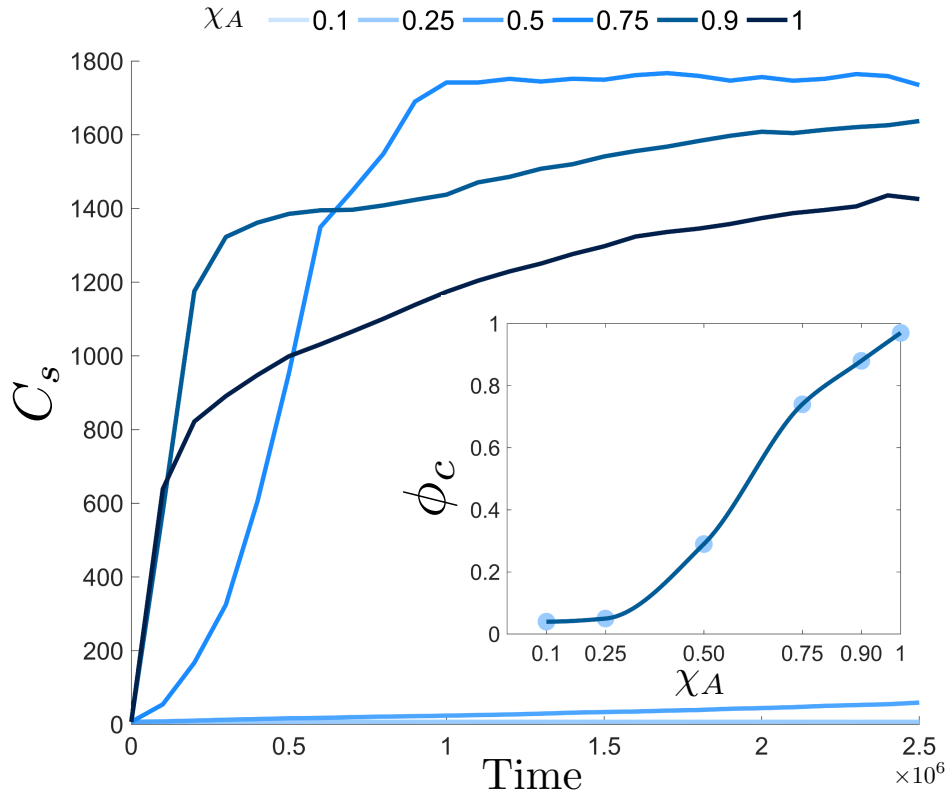


FIG. 7. Cluster analysis for different fractions  $\chi_A$  of active particles at fixed  $\rho = 0.05$ . Cluster size and fraction of particles in clusters as in Fig. 6 for different  $\chi_A$  in a binary mixture of active and passive crowders.

in Fig. 7), likely because initially the rapid directional change of the passive particles randomizes the motion of the active particles. Eventually, however, clustering sets in. While clustering sets in later for  $\chi_A = 0.75$  than for  $\chi_A = 1$ , it reaches its stationary state faster.

Above we have shown a correspondence between the onset of clustering and a decrease of the enhanced diffusion of a passive tracer (Fig. 5). Since clustering is decreased by increasing the fraction of passive particles in the system, we expect that the decrease in diffusion of the tracer is less pronounced when passive particles are present. This is indeed the case, as shown in Fig. 8, where we plot the diffusion coefficient as a function of the density for different combinations of the tumbling probability  $\alpha$  and the fraction of active crowders  $\chi_A$ : decreasing the fraction of active crowders leads to a broader peak in the diffusion coefficient as a function of density. We interpret this observation as reflecting the fact that a larger fraction of the active particles is in the gas phase and can push the tracer. At the same time, however, the value of the maximal diffusion coefficient is also decreased, reflecting the fact that the total number of active particles is reduced. Nevertheless, even for very low fractions of active particles (bottom row in Fig. 8), the diffusion coefficient is still increased compared to the case with only passive particles. For instance, for  $\alpha = 0.1$ ,  $\chi_A = 0.1$ , it is increased up to 5-fold.

#### IV. CONCLUSION

In this study, we have analyzed the diffusion of a tracer particle in a crowded active system using a minimal lattice model. We implemented the pushing of a passive tracer by active crowder particles by a simple collision rule. A passive tracer in an otherwise purely active system or in a binary mixture of active and passive particles exhibits different motility regimes including significantly enhanced effective diffusion. Our results show that the extent to which diffusion is enhanced depends on the activity of the crowder particles (modulated via their hopping rate relative to the tracer's hopping rate and via their tumbling probability, i.e. via the persistence of their motion) and on their density. The interplay of activity and density depends on the dynamics of the particles directly, but also indirectly via the phase separation of the crowders into low-density (gas-phase) regions and dense clusters. The latter has a negative effect on the mobility of the tracer, both when the tracer becomes trapped in a cluster and when the tracer



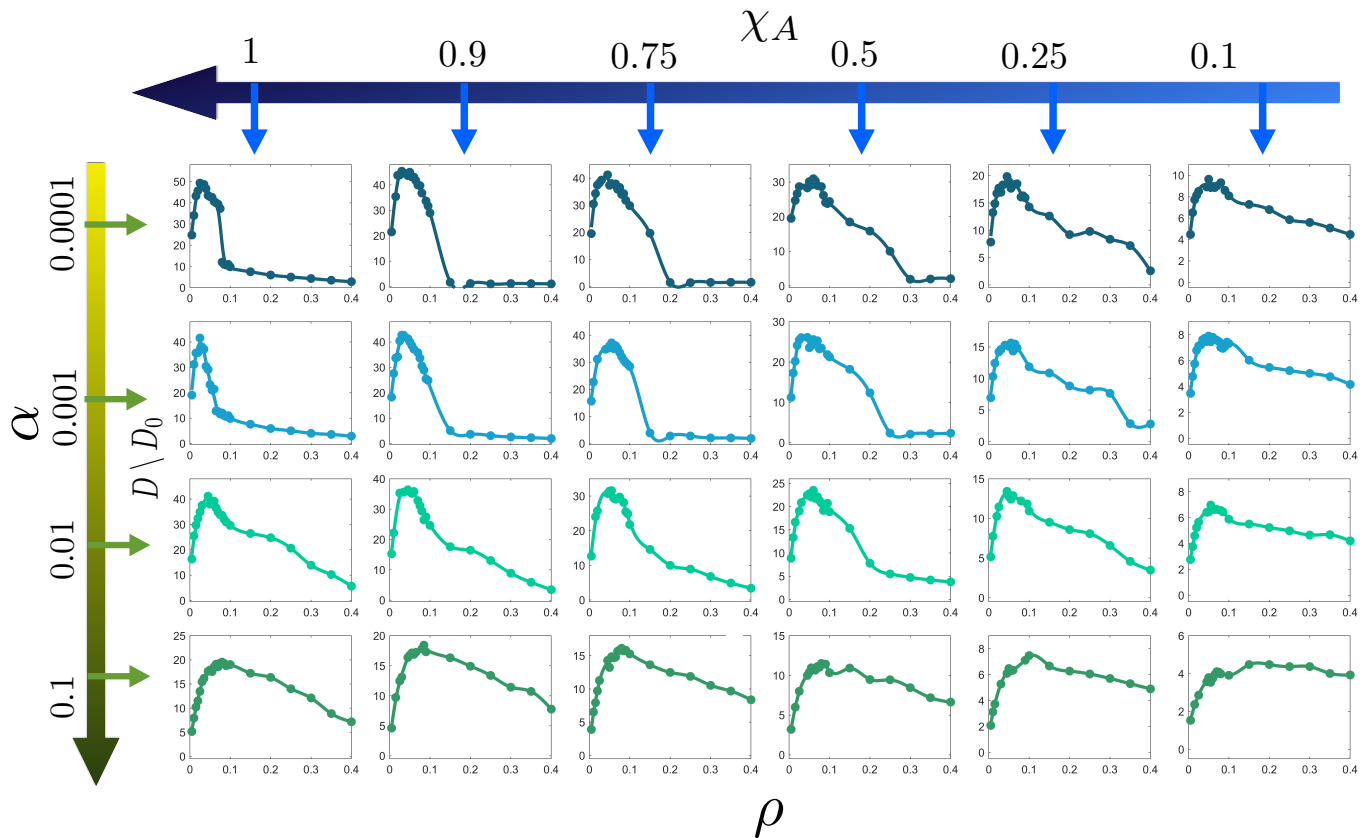


FIG. 8. The diffusion coefficient of a tracer with  $\beta = 0.9$  as a function of the density  $\rho$  and of the fraction of active crowders  $\chi_A$  in a binary mixture.

moves in a low-density area, where it is not pushed by active particles. Our findings point to an intricate interplay between the local dynamics of enhanced tracer diffusion and the global dynamics of the system. Given the simplicity of our model, one can extend it to other collision rules among the particles as well as use it to study the impact of active crowding on other physical processes.

#### ACKNOWLEDGEMENT

This research was conducted within the Max Planck School Matter to Life supported by the German Federal Ministry of Education and Research (BMBF) in collaboration with the Max Planck Society. The authors acknowledge further support by DFG through SFB 937 project A21 in the initial phase of this work.

- 
- [1] R. John Ellis, “Macromolecular crowding: obvious but underappreciated,” *Trends in biochemical sciences* **26**, 597–604 (2001).
  - [2] James A. Dix and A.S. Verkman, “Crowding effects on diffusion in solutions and cells,” *Annual Review of Biophysics* **37**, 247–263 (2008).
  - [3] Clemens Bechinger, Roberto Di Leonardo, Hartmut Löwen, Charles Reichardt, Giorgio Volpe, and Giovanni Volpe, “Active particles in complex and crowded environments,” *Rev. Mod. Phys.* **88**, 045006 (2016).
  - [4] Stefan Klumpp, William Bode, and Palka Puri, “Life in crowded conditions,” *The European Physical Journal Special Topics*, 1–14 (2019), <https://doi.org/10.1140/epjst/e2018-800088-6>.
  - [5] S B Zimmerman and A P Minton, “Macromolecular crowding: Biochemical, biophysical, and physiological consequences,” *Annual Review of Biophysics and Biomolecular Structure* **22**, 27–65 (1993).
  - [6] Neil H. Mendelson, Adrienne Bourque, Kathryn Wilkening, Kevin R. Anderson, and Joseph C. Watkins, “Organized cell swimming motions in bacillus subtilis colonies: Patterns of short-lived whirls and jets,” *American Society for Microbiology*

*Journals* **181**, 600–609 (1999).

- [7] Luanne Hall-Stoodley, J William Costerton, and Paul Stoodley, “Bacterial biofilms: from the natural environment to infectious diseases,” *Nature reviews microbiology* **2**, 95–108 (2004), <https://doi.org/10.1038/nrmicro821>.
- [8] Guillaume Salbreux and Frank Jülicher, “Mechanics of active surfaces,” *Phys. Rev. E* **96**, 032404 (2017).
- [9] Daisuke Mizuno, Catherine Tardin, Christoph F Schmidt, and Frederik C MacKintosh, “Nonequilibrium mechanics of active cytoskeletal networks,” *Science* **315**, 370–373 (2007).
- [10] M. J. I. Muller, S. Klumpp, and R. Lipowsky, “Tug-of-war as a cooperative mechanism for bidirectional cargo transport by molecular motors,” *Proceedings of the National Academy of Sciences* **105**, 4609–4614 (2008).
- [11] Christian B. Korn, Stefan Klumpp, Reinhard Lipowsky, and Ulrich S. Schwarz, “Stochastic simulations of cargo transport by processive molecular motors,” *The Journal of Chemical Physics* **131**, 245107 (2009), <https://doi.org/10.1063/1.3279305>.
- [12] Ramin Golestanian, “Anomalous diffusion of symmetric and asymmetric active colloids,” *Physical Review Letters* **102** (2009), [10.1103/physrevlett.102.188305](https://doi.org/10.1103/physrevlett.102.188305).
- [13] P. Illien, T. Adeleke-Larodo, and R. Golestanian, “Diffusion of an enzyme: The role of fluctuation-induced hydrodynamic coupling,” *EPL (Europhysics Letters)* **119**, 40002 (2017).
- [14] Andrey Sokolov and Igor S. Aranson, “Physical properties of collective motion in suspensions of bacteria,” *Phys. Rev. Lett.* **109**, 248109 (2012).
- [15] Jörn Dunkel, Sebastian Heidenreich, Knut Drescher, Henricus H. Wensink, Markus Bär, and Raymond E. Goldstein, “Fluid dynamics of bacterial turbulence,” *Phys. Rev. Lett.* **110**, 228102 (2013).
- [16] Michael C Konopka, Kem A Sochacki, Benjamin P Bratton, Irina A Shkel, M Thomas Record, and James C Weissshaar, “Cytoplasmic protein mobility in osmotically stressed escherichia coli,” *Journal of bacteriology* **191**, 231–237 (2009).
- [17] Bradley R Parry, Ivan V Surovtsev, Matthew T Cabeen, Corey S O’Hern, Eric R Dufresne, and Christine Jacobs-Wagner, “The bacterial cytoplasm has glass-like properties and is fluidized by metabolic activity,” *Cell* **156**, 183–194 (2014).
- [18] Arnold J Boersma, Inge S Zuhorn, and Bert Poolman, “A sensor for quantification of macromolecular crowding in living cells,” *Nature methods* **12**, 227 (2015).
- [19] David Gnuttt, Mimi Gao, Oliver Brylski, Matthias Heyden, and Simon Ebbinghaus, “Excluded-volume effects in living cells,” *Angewandte Chemie International Edition* **54**, 2548–2551 (2015).
- [20] Donald L Koch and John F Brady, “Anomalous diffusion in heterogeneous porous media,” *The Physics of fluids* **31**, 965–973 (1988).
- [21] Surya K Ghosh, Andrey G Cherstvy, Denis S Grebenkov, and Ralf Metzler, “Anomalous, non-gaussian tracer diffusion in crowded two-dimensional environments,” *New Journal of Physics* **18**, 013027 (2016).
- [22] Xiao-Lun Wu and Albert Libchaber, “Particle diffusion in a quasi-two-dimensional bacterial bath,” *Phys. Rev. Lett.* **84**, 3017–3020 (2000).
- [23] Guillaume Grégoire, Hugues Chaté, and Yuhai Tu, “Active and passive particles: Modeling beads in a bacterial bath,” *Phys. Rev. E* **64**, 011902 (2001).
- [24] Irwin M Zaid, Jörn Dunkel, and Julia M Yeomans, “Lvy fluctuations and mixing in dilute suspensions of algae and bacteria,” *Journal of the Royal Society, Interface* **8**, 13141331 (2011), <https://doi.org/10.1098/rsif.2010.0545>.
- [25] Chantal Valeriani, Martin Li, John Novosel, Jochen Arlt, and Davide Marenduzzo, “Colloids in a bacterial bath: simulations and experiments,” *Soft Matter* **7**, 5228–5238 (2011).
- [26] Dmitri O. Pushkin and Julia M. Yeomans, “Fluid mixing by curved trajectories of microswimmers,” *Phys. Rev. Lett.* **111**, 188101 (2013).
- [27] Rodrigo Soto and Ramin Golestanian, “Run-and-tumble dynamics in a crowded environment: Persistent exclusion process for swimmers,” *Phys. Rev. E* **89**, 012706 (2014).
- [28] TV Kasyap, Donald L Koch, and Mingming Wu, “Hydrodynamic tracer diffusion in suspensions of swimming bacteria,” *Physics of Fluids* **26**, 081901 (2014), <https://doi.org/10.1063/1.4891570>.
- [29] Alexander Morozov and Davide Marenduzzo, “Enhanced diffusion of tracer particles in dilute bacterial suspensions,” *Soft Matter* **10**, 2748–2758 (2014).
- [30] Yuguang Yang and Michael A. Bevan, “Cargo capture and transport by colloidal swarms,” *Science Advances* **6** (2020), [10.1126/sciadv.aay7679](https://doi.org/10.1126/sciadv.aay7679).
- [31] Avi Caspi, Rony Granek, and Michael Elbaum, “Enhanced diffusion in active intracellular transport,” *Phys. Rev. Lett.* **85**, 5655–5658 (2000).
- [32] Min Jun Kim and Kenneth S. Breuer, “Enhanced diffusion due to motile bacteria,” *Physics of Fluids* **16**, L78–L81 (2004), <https://doi.org/10.1063/1.1787527>.
- [33] Kyriacos C. Leptos, Jeffrey S. Guasto, J. P. Gollub, Adriana I. Pesci, and Raymond E. Goldstein, “Dynamics of enhanced tracer diffusion in suspensions of swimming eukaryotic microorganisms,” *Phys. Rev. Lett.* **103**, 198103 (2009).
- [34] Gastón Miño, Thomas E. Mallouk, Thierry Darnige, Mauricio Hoyos, Jeremi Dauchet, Jocelyn Dunstan, Rodrigo Soto, Yang Wang, Annie Rousselet, and Eric Clement, “Enhanced diffusion due to active swimmers at a solid surface,” *Phys. Rev. Lett.* **106**, 048102 (2011).
- [35] G. L. Mio, J. Dunstan, A. Rousselet, E. Clment, and R. Soto, “Induced diffusion of tracers in a bacterial suspension: theory and experiments,” *Journal of Fluid Mechanics* **729**, 423444 (2013).
- [36] Alys Jepson, Vincent A. Martinez, Jana Schwarz-Linek, Alexander Morozov, and Wilson C. K. Poon, “Enhanced diffusion of nonswimmers in a three-dimensional bath of motile bacteria,” *Phys. Rev. E* **88**, 041002 (2013).
- [37] N Koumakis, A Lepore, C Maggi, and R Di Leonardo, “Targeted delivery of colloids by swimming bacteria,” *Nature communications* **4**, 1–6 (2013), <https://doi.org/10.1038/ncomms3588>.

- [38] L. Angelani, C. Maggi, M. L. Bernardini, A. Rizzo, and R. Di Leonardo, “Effective interactions between colloidal particles suspended in a bath of swimming cells,” *Phys. Rev. Lett.* **107**, 138302 (2011).
- [39] Surya K Ghosh, Andrey G Cherstvy, and Ralf Metzler, “Non-universal tracer diffusion in crowded media of non-inert obstacles,” *Physical Chemistry Chemical Physics* **17**, 1847–1858 (2015).
- [40] O Bénichou, P Illien, G Oshanin, A Sarracino, and R Voiturier, “Tracer diffusion in crowded narrow channels,” *Journal of Physics: Condensed Matter* **30**, 443001 (2018).
- [41] Carlos Mejia-Monasterio, Sergei Nechaev, Gleb Oshanin, and Oleg Vasilyev, “Tracer diffusion on a crowded random manhattan lattice,” *New Journal of Physics* **22**, 033024 (2020).
- [42] Eric W. Burkholder and John F. Brady, “Tracer diffusion in active suspensions,” *Phys. Rev. E* **95**, 052605 (2017).
- [43] O. M. Braun and C. A. Sholl, “Diffusion in generalized lattice-gas models,” *Phys. Rev. B* **58**, 14870–14879 (1998).
- [44] Vyas Ramasubramani, Bradley D. Dice, Eric S. Harper, Matthew P. Spellings, Joshua A. Anderson, and Sharon C. Glotzer, “freud: A software suite for high throughput analysis of particle simulation data,” (2019), [arXiv:1906.06317](https://arxiv.org/abs/1906.06317).